# Statistical instability of barrier microdischarges operating in townsend regime

V. P. Nagorny[a)]
*Plasma Dynamics Corporation, Waterville, Ohio 43566-1062*

(Received 10 July 2006; accepted 1 November 2006; published online 17 January 2007)

The dynamics of barrier microdischarges operating in a Townsend regime is studied analytically and via kinetic particle-in-cell/Monte Carlo simulations. It is shown that statistical fluctuations of the number of charged particles in the discharge gap strongly influence the dynamics of natural oscillations of the discharge current and may even lead to a disruption of the discharge. Analysis of the statistical effects based on a simple model is suggested. The role of external sources in stabilizing microdischarges is clarified. © *2007 American Institute of Physics*.
[DOI: 10.1063/1.2425196]

## I. INTRODUCTION

The term "Townsend" or "dark" discharge is usually referred to as a very weak self-sustaining discharge, when the discharge current is low (due to resistive limiter in the electric circuit) and the voltage across the p1ane gap is close to the breakdown voltage. In fact, the ion density in such a discharge is so low that electric field in the gap remains practically undistorted by the charges. Depending on the parameters of the external circuit, the Townsend discharge can be unstable (so that it eventually transforms in to a glow discharge) or stable (so that after some transient processes the discharge current approaches its stationary value). The stationary current $I_0$ in the case when it is limited by a resistor is equal to $I_0=(V_{\text{appl}}-V_{\text{br}})/R$, where $V_{\text{appl}}$ and $V_{\text{br}}$ are applied and breakdown voltages, respectively, and $R$ is the limiting resistor. Discharges operating in Townsend regime are being investigated for many applications (plasma actuators, thin film depositions, sterilization of biological systems, etc.), and are currently widely used in plasma display industry for the setup of plasma display panel (PDP) cells before addressing.[1,2] In all these applications, electrodes are covered with a dielectric, so the stationary current regime is reached by applying a slowly increasing or decreasing (ramping) voltage to one of the electrodes, and the stationary value of the current is

$$I_0 = CdV_{\text{appl}}/dt, \tag{1}$$

where $C$ is the capacitance of the dielectric, covering electrodes. We investigated earlier[2] the dynamics of such "ramp" discharge, both numerically and analytically using hydrodynamic approximation and found that its behavior follows Hamiltonian type of equations. The stationary discharge establishes through a series of current/density oscillations, which in the one-dimensional (1D) case can be described analytically.[2] The amplitude and the depth of these oscillations depend on the initial conditions. If the initial conditions are close to the stationary ones ($\exp|\ln[I(0)/I_0]|-1 \ll 1$, when $V_{\text{disch}}=V_{\text{br}}$), then the amplitude of these oscillations is small compared to $I_0$, and it is large otherwise. Later these results were confirmed in various experiments with dielectric barrier discharges.[3–6] It is interesting to note that even in more general than described here case, with a complicated external circuit (which has resistive, inductive, and capacitive elements), this highly dissipative system is still governed by Hamiltonian equations![7]

According to the hydrodynamic theory, both large oscillation and large voltage ramp rate ($|dV/dt|$) can lead to instability of the Townsend discharge, but if initial conditions are good and the ramp rate is low then the discharge is steady and stable.

In this paper we point out that quite often (as in a PDP cell) the number of particles participating in the Townsend discharge is relatively small—some thousands to tens of thousands of particles. This causes emerging kind of effects, which fluid approximation completely ignores statistical ones, and which should be investigated. As it turned out, these effects are indeed very important, especially for low ramp rates, and gases with low secondary emission coefficient from the surface material. We discovered that for conditions of the Townsend discharge in a PDP cell, fluctuations of the number of ions in the gap $N$ (and current) can significantly exceed the statistical expectation of $\sqrt{N}$, they lead to instability of the stationary discharge, and eventually to its extinguishing. Opposite to a large size discharge, the priming plays much less important role in a microdischarge, but the role of independent sources, such as exoemission, in stabilizing the discharge increases very much.

The statistical instability behaves not like a regular instability, where a small initial fluctuation/distortion grows exponentially. Instead, every fluctuation here does not grow, but changes the discharge conditions leading to oscillations of the current and ion density. The series of uncorrelated fluctuations leads to large oscillations and ultimately to the extinguishing of the discharge.

The plan of this paper is as follows. In Sec. II we briefly summarize our theory of the ramp discharge based on the fluid approximation, and show typical results of fluid simulations. In Sec. III we show the results of three-dimensional (3D) simulations of the Townsend discharge in a PDP cell

[a)]Present address: Mattson Technology, Inc., 47131 Bayside Pkwy, Fremont, CA 94538; electronic mail: vnagorny@plasmadynamics.com

 

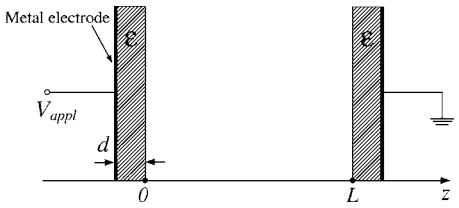


FIG. 1. Basic geometry (1D) of the barrier discharge setup. Positive $z$ direction is chosen from the anode toward the cathode.

with a limited number of particles obtained with our 3D particle-in-cell/Monte Carlo code, and analyze them. We will show that fluid equations may display similar behavior if one modifies them to include statistical effects. In Sec. IV we investigate the stabilizing effects of independent sources of electrons, and compare the effects from different sources. Finally, in Sec. V we make a few summation remarks.

## II. HYDRODYNAMIC CONSIDERATION

To avoid unnecessary complications we limit this consideration to a one-dimensional discharge between plane electrodes covered with dielectric layers of a thickness $d$ and with dielectric constant $\varepsilon$ (see Fig. 1). The growth or decay of the current is determined by the balance between production of particles in the gap and their losses. In case when all losses are small compared to those to the walls and avalanche is controlled by the secondary emission of electrons from the cathode surface, this balance can be determined by the parameter $\Delta_T$ defined as

$$\Delta_T = \gamma\left\{\exp\int[\alpha(E)dx] - 1\right\} - 1, \tag{2}$$

where $\alpha$ and $\gamma$ are the first and the second Townsend coefficients, and $L$ is the gap length (see Fig. 1). If $N$ is the number of ions in the gap, then $N\Delta_T$ is equal to the number of extra ions in the gap in the following generation separated from the current one by the ion transit time $\tau \sim L/v_i$, where $v_i$ is the ion velocity, so one can write the equation for the electron current at the cathode ($x=L$) as

$$\frac{\partial j_e(L,t)}{\partial t} = \frac{\nu_i}{L}\Delta_T j_e(L,t). \tag{3}$$

If $\Delta_T > 0$, the current grows, if $\Delta_T < 0$, the current decays, and $\Delta_T = 0$ determines the stationary condition and the breakdown voltage. Near the breakdown, the absolute value of $\Delta_T$ is small $|\Delta_T| \ll 1$ and thus the current and ion density change in the system with a characteristic time

$$\tau \sim (L/\nu_i)/\Delta_T, \tag{4}$$

significantly exceeding the ion transit time. This means that ions leave the gap much faster than they change their density, so they do not accumulate in the gap, and one can neglect the spatial variation of the electric field in the gap. In this case the total particle current $j = j_e + j_i$ is independent of the coordinate $x$ along the gap $j = j(t) = kj_e(L,t)$, where $k = (1+\gamma)/\gamma = \text{const}$. Expanding $\Delta_T$ in Eq. (3) in Taylor series around $V = V_{\text{br}}$, and using total current $j$ instead of $j_e$, one obtains[2,8]

$$\frac{\partial j}{\partial t} = \frac{\kappa}{L}(V - V_{\text{br}})j, \tag{5}$$

where $\kappa = v_i(\partial\Delta_T/\partial V)|_{V=V_{\text{br}}} \sim v_i(\partial\alpha/\partial E)|_{E=E_{\text{br}}}$ and $E_{\text{br}} \equiv V_{\text{br}}/L$. The equation for electric field in the ramp discharge is[2]

$$\frac{\partial V}{\partial t} = -C^{-1}(j - j_{\text{dc}}), \tag{6}$$

where $C \sim \varepsilon/(8\pi d)$ is the capacitance of the dielectric and $j_{\text{dc}} = CdV_{\text{appl}}/dt$. As it should, the stationary solution of Eqs. (5) and (6) is

$$V = V_{\text{br}}, \quad j(t) = j_{\text{dc}}. \tag{7}$$

One can rewrite Eqs. (5) and (6) in the form of Hamilton's equations, for a particle of "mass" $m^* = L/(\kappa V_{\text{br}})$, "momentum" $p = (V - V_{\text{br}})/V_{\text{br}}$, and "coordinate" $q = \ln(j/j_{\text{dc}})$,

$$\dot{q} = p/m^* = \frac{\kappa V_{\text{br}}}{L}p = \frac{\partial H(p,q)}{\partial p},$$

$$\dot{p} = (\lambda/V_{\text{br}})(1 - e^q) = -\frac{\partial U}{\partial q} = -\frac{\partial H(p,q)}{\partial q}, \tag{8}$$

where

$$H(p,q) = p^2/2m^* + U(q), \quad U(q) = \frac{\lambda}{V_{\text{br}}}(e^q - q - 1) \tag{9}$$

are the Hamiltonian of the system, and the "potential" $\lambda = dV_{\text{appl}}/dt$ is the ramp rate, and we have chosen the constant, so that $U(0) = 0$.

The energy integral of Eqs. (8)

$$W = H(p,q) = \frac{p^2}{2m^*} + \frac{\lambda}{V_{\text{br}}}(e^q - q - 1) = \text{const} \tag{10}$$

describes periodic oscillations in the potential $U(q)$ which has minimum at $q=0$, so the "particle" oscillates between points $q_{\min}(W) < 0$ and $q_{\min}(W) > 0$ (see Fig. 2). The period $T$ of current oscillations

$$T = \oint \frac{dq}{\sqrt{(2/m^*)[W - U(q)]}} \tag{11}$$

depends on their energy $W$. When oscillations are small they become harmonic ones of a frequency $\omega_0$,

$$\omega_0^2 = \lambda\kappa/L \sim (\nu_i\lambda/L)(\partial\alpha/\partial E)|_{E=E_{\text{br}}}. \tag{12}$$

When oscillations are large, $T$ is determined by the linear part of $U(q)$ (when the current is small), and it increases with the amplitude of oscillations

$$T \sim 2\sqrt{2Wm^*}(V_{\text{br}}/\lambda) \sim 2\sqrt{2L/(\kappa\lambda)}\sqrt{j_{\max}/j_{\text{dc}}}$$
$$\sim 3\sqrt{j_{\max}/j_{\text{dc}}}/\omega_0.$$

It is useful to note that $p_{\max}\kappa/L$ is a characteristic frequency $\Omega$ of the pulse when the constant voltage is applied to the gap[8] (the pulse half-width $\tau_{1/2} = 3.52/\Omega$), and $\lambda/2p_{\max}$ is the inverse time, required to restore the voltage for the

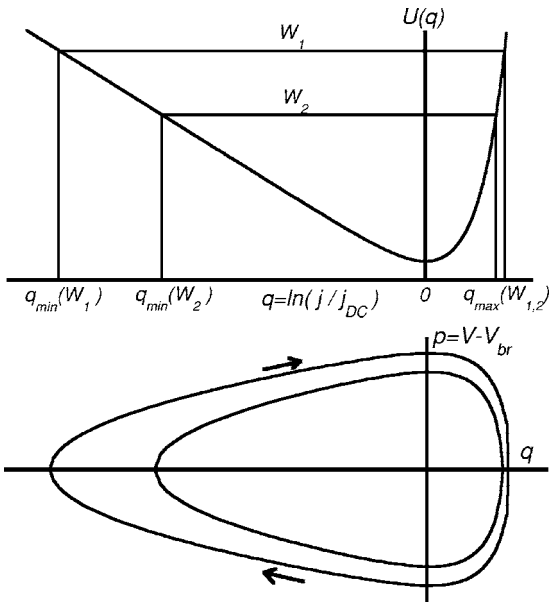


FIG. 2. Function $U(q)$ and phase trajectories. The two horizontal lines show two different values of the energy $W=W_1$, $W=W_2$, and $W_1>W_2$. The larger oscillations of a current (higher peaks and lower dips) correspond to the larger energy.

next pulse. As the "energy" (and $p_{\max}$) increases, the period of oscillations increases too, while the half-width of the pulses decreases.

Both extremes obviously occur at $p=0$ ($V=V_{\rm br}$), so with any priming $[q(t=0)]$ oscillations are smaller if $p(t=0)=0$ or $V(0)=V_{\rm br}$. For large current oscillations $(\exp|q_{\max,\min}| \gg |q_{\max,\min}|+1)$ we obtain $W=-\lambda q_{\min}=\lambda e^{q_{\max}}$ or

$$j_{\max}=j_{\rm dc}\ln(j_{\rm dc}/j_{\min}), \tag{13}$$

which shows that smaller ramp rates and better priming (larger $j_{\min}$) result in smaller oscillations. It also shows that even moderate current peaks are being followed by large current deeps.

In the presence of metastable atoms, photoionization, or electron exoemission from the surface[9–11] these oscillations decay.[2,6] The reason for this is the presence of independent (weak) source, which mainly affects the minimum current, increasing it and thus affecting the amplitude of oscillations. Assuming that the source is weak, one can evaluate the decrement of the oscillations due to such a source, including it in Eqs. (8), and then calculating the change of the "energy" of the oscillation during one oscillation period,

$$\dot q=\frac{p}{m^*}+\frac{e}{\tau_i j}\hat S, \tag{14}$$

where $\hat S$ is the production of electrons and ions in the gap initialized by any of these sources per ion transit time with account of the following electron avalanches. For example, if the power of the source is $S(z,t)$, and $e^{\alpha L}\gg 1$, then with account of electron avalanches, $\hat S\approx(\alpha e^{\alpha L})^{-1}\int_0^L S(z,t)e^{\alpha L}dz$ (see Appendix).

Obviously, in the presence of external sources, the stationary value of $V$ (or $p$) changes. The new stationary value of $V$ is determined from Eq. (14), which gives

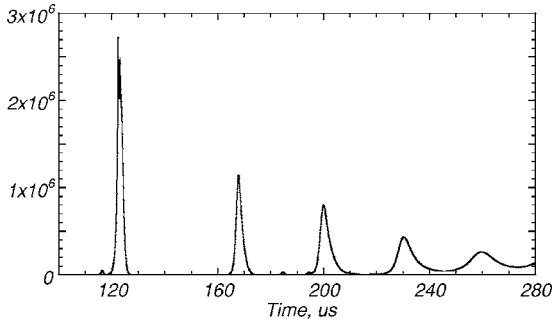


FIG. 3. The number of ions in a PDP cell during the ramp discharge (3D fluid simulations), when initial density is significantly lower than necessary to sustain a stationary current. After the first peak the ion density became so low [see Eq. (13)] that the number of particles in the cell is less than 1 and is not seen on a linear scale. Continuous approach (based on density) though does not result in extinguishing of the discharge. Eventually current grows, and after some number of smaller oscillations the current stabilizes at $j=j_{\rm dc}$. This indicates that continuous approach may not always be adequate for small systems such as PDP cell.

$$V=V'_{\rm br}=V_{\rm br}-\delta V_{\rm br}\equiv V_{\rm br}-\frac{eL}{\kappa\tau_i j_{\rm dc}}\bar S, \tag{15}$$

where $\bar S\equiv\hat S(V=V_{\rm br},j=j_{\rm dc})$. However, if one changes variable $p=(V-V_{\rm br})/V_{\rm br}$ to $p'=(V-V'_{\rm br})/V_{\rm br}$ then equations for $p'$ and $q$ will be the same as the original equations for $p$ and $q$, except for the source in the new equation for $\dot q$,

$$\dot q=\frac{p'}{m^*}+\frac{e}{\tau_i}\left(\frac{\hat S}{j}-\frac{\bar S}{j_{\rm dc}}\right). \tag{16}$$

Taking time derivative of the energy $W=H(p',q)$ we obtain

$$\frac{dW}{dt}\equiv\frac{d}{dt}\left[\frac{p'^2}{2m^*}+\frac{\lambda}{V_{\rm br}}(e^q-q-1)\right]=-\frac{e}{\tau_i}\left(\frac{\hat S}{j}-\frac{\bar S}{j_{\rm dc}}\right)\dot p' \tag{17}$$

and thus

$$\delta W_t^{t+T}=-\frac{e}{\tau_i}\oint_{C(W)}\frac{S\dot p'dt}{j}\approx-\frac{e\bar S}{\tau_i}\oint_{C(W)}\frac{dp'}{j}<0, \tag{18}$$

where $C(W)$ is the trajectory in the $(p',q)$ phase space, and we used that $\oint dp'=0$. The inequality (18) is provided by the fact that the current is smaller, where $dp'>0$, and larger, where $dp'<0$. For small oscillations this gives the rate of decay $\nu$ ($W\propto e^{-\nu t}$),

$$\nu=\frac{e\bar S}{j_{\rm dc}\tau_i}. \tag{19}$$

Oscillations may also decay, due to resistive impedance of the positive column, or external resistor. There are other factors that may cause decay or increase of oscillations,[7] but they are beyond the scope of this paper. Typical behavior of the number of ions in the gap of a PDP cell during the ramp discharge is shown in Fig. 3.

One should remember, though, that if the ramp rate is high, then the ion density in the gap ($n_i\propto j_i/v_i$) may be large enough to affect the electric field. And if this results in decreasing of the electric field near the anode by about $\delta E_a$

$\geqslant E_{\mathrm{br}} \approx V_{\mathrm{br}}/L$, then the Townsend mode of the discharge with constant current cannot exist—instead, a series of strong discharge pulses (see Ref. 12) with the average current equal to $CdV_{\mathrm{appl}}/dt$ replaces it. This gives the estimate for the upper limit of the ramp rate $\lambda_{\max}$,

$$\frac{dV_{\mathrm{appl}}}{dt} < \frac{2d}{L\varepsilon}\mu_i E_{\mathrm{br}}^2 = \frac{2d}{L^3\varepsilon}\mu_i V_{\mathrm{br}}^2 \equiv \lambda_{\max}, \tag{20}$$

where $\mu_i$ is ion mobility. Since the breakdown voltage either decreasing or slowly increasing function of $L$ the maximum ramp rate decreases with the increase of gap length. Everywhere below we will assume that the ramp rate is small compared to $\lambda_{\max}$.

## III. STATISTICAL INSTABILITY OF A TOWNSEND DISCHARGE

When fluid approximation is used it is implicitly assumed that the number of particles participating in the discharge is very large, and statistical fluctuations are negligibly small. However today's technology is often based on using so small elements that such assumption is no longer valid. For example, the average number of ions $\langle N\rangle$ in the gap during the ramp discharge is about

$$\langle N\rangle \approx (\tau_i/2)CdV/dt, \tag{21}$$

and for typical parameters of a plasma display cell ($C \sim 0.02$ pF, $\tau_i \sim 150$ ns, and $dV/dt \sim 1-3$ V/$\mu$s) it gives $\langle N\rangle \sim 15\,000-60\,000$. During the current oscillations, $N$ is even lower, and statistical fluctuations may not be ignored. To investigate statistical effects we use a Monte Carlo approach, which properly takes into account the statistical nature of the processes responsible for the production of charged particles in the gap (secondary electron emission and ionizing collisions).

The transverse dimensions of the cell in such a setup are not important so we choose dimensions of the test cell similar to those in a plasma display cell. Specifically, we use transverse dimension $100\times 100$ $\mu$m$^2$, the gap length $L=90-100$ $\mu$m and the capacitance of the dielectric covering electrodes varies around 0.03 pF.

We used mixtures of Ne and Xe gases instead of a hypothetical gas, as they are of a particularly high interest to plasma display industry, and because by changing the ratio of Xe to Ne one can easily change the effective secondary emission coefficient[13,14] of the mixture and investigate the effects of $\gamma$ on the stability of the discharge. The specific vacuum values of secondary emission coefficients are often not known, so for our goals we have used large coefficient for Ne, $\gamma_{\mathrm{Ne}}=0.64$, and small coefficient for Xe, $\gamma_{\mathrm{Xe}}=0.001-0.1$. As we have found, the secondary emission coefficient does indeed very strongly affect the amplitude of fluctuations and the discharge stability.

We start all ramps at $t=0$ with the voltage equal (or close) to the breakdown voltage, injecting from the cathode $\sim\gamma\langle N\rangle$ electrons, so that they produce in the gap the number of ions close to the one given by Eq. (21). One should note that because of a small ion transit time compared to the period of oscillations, the initial ion profile is not of a large importance—any difference from the stationary profile would result in some noise lasting for just a few ion transit times, but will not lead to large oscillations. In the absence of fluctuations the initial conditions we have chosen would result in small weakly decaying oscillations, so one can assume that any difference in the discharge behavior is caused by fluctuations.

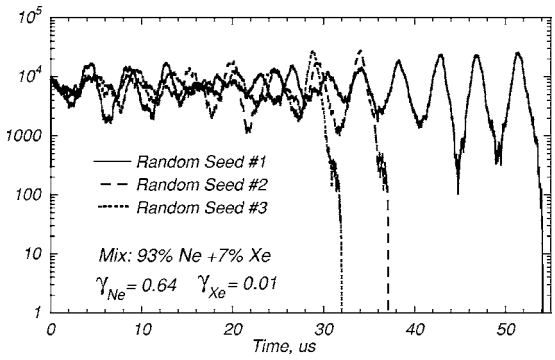


FIG. 4. Three simulations of the ramp discharge started with identical "ideal" initial conditions but using different sequences of random numbers, which control the specific order of microscopic events—secondary electron emission and collisions. Fluctuations are clearly responsible for variations of the amplitude of the oscillations. If at any moment Monte Carlo simulations were replaced by fluid simulations, they would show steady, slow decaying oscillations from that moment on.

Figure 4 shows the number of ions in the gap in the ramp discharge started at almost ideal initial conditions ($V=V_{\mathrm{br}}$, $N=\langle N\rangle$, $V$—voltage across the gap). One can see that there is no regularity in the variation of the amplitude of oscillations. It increases or decreases, depending on the sequence and the magnitude of fluctuations rather than on macroscopic discharge conditions. Opposite to the fluid theory, which predicts constant number of ions for such initial conditions, not only oscillations have appeared, but also the number of ions in the gap oscillated until they completely disappeared. As one can see the change of the "seed" number initiating the random sequence, which microscopically controls random events such as ionization and secondary emission, has a much stronger effect on the discharge than the initial conditions.

These random sequences describe actual random events such as secondary emission or ionization collisions, which continuous (both fluid and Boltzmann kinetics) approaches consider deterministically. For example, in the fluid consideration the secondary emission coefficient $\gamma=0.01$ means that electron flux from the cathode is at all times a hundred times smaller than the ion flux to it, independently of how many actual ions arrive to it. In the Monte Carlo consideration (as in real discharge), when ion arrives to the surface, it does not produce 0.01 electron. This coefficient $\gamma$ describes only the probability of the electron emission. Actual electron may be emitted after the 1st, 21st, or 200th ion arriving to that surface. Similar probability consideration applies to the excitation and ionization events. Fluctuations by themselves normally do not lead to a large deviation from the original condition ($\delta N \sim \sqrt{N}$), but in the case of a Townsend discharge, where successful generations of particles are linked $[j_e(L,t)=\gamma j_i(L,t), \quad j_i(L,t)=\int_0^L \alpha(t-x/v_i)j_e(L-x,t-x/v_i)dx,$

see Appendix and Ref. 8], they lead to a regular "diffusion" of the number of particles participating in the discharge $N(t+n\tau_i)=N(t)+\Sigma_1^n \delta N_k$ and the current. Here $\delta N_k$ is a fluctuation of the number of ions produced in $k$'s generation.

Of course, if $\delta N_k$ are small then the time required for significant change of the value of $N$ may become very large and other processes are more important than diffusion. So let us now estimate the magnitude of fluctuations $\delta N$ in a Townsend discharge. Since particles do not affect the electric field in the gap, and the characteristic time of the macroscopic changes is large compared to the ion transit time [see Eq. (4)] one can analyze fluctuations (and the dynamics of the discharge) in terms of the number of particles in subsequent generations. Ideally, the number of ions in the gap stays close to $\langle N\rangle$, Eq. (21), which is provided by the balance between secondary emission ($\gamma$) and amplification in the avalanche [$\sim\exp(\alpha L)\sim 1/\gamma$]. In reality both processes have statistical nature, which means that the number of secondary electrons emitted from the surface is not exactly $\gamma N$, but has fluctuations with dispersion of the order of $\sqrt{\gamma N}$. After the avalanche with amplification factor $\sim 1/\gamma$, the number of ions in the gap differs from the original one by $\delta N\sim\sqrt{N/\gamma}$. So the relative fluctuation $\delta N/N\sim 1/\sqrt{\gamma N}$ can be very large when $N$ or $\gamma$ are small. The second statistical process is the avalanche. Fluctuations due to this process have the same order of magnitude $\delta N\sim(1/2)\exp(\alpha L)\sqrt{\gamma N}\sim\sqrt{N/\gamma}$. This result explains why the role of fluctuations is so significant—$\delta N/N$ can easily be about 0.1–1 (or even larger than 1) in the minima of the current oscillations. Since $\gamma$ depends on the gas mixture, one should expect larger fluctuations in mixtures with larger xenon component, where effective $\gamma$ is very small. This consideration shows the importance of the secondary emission coefficient for statistical properties of the discharge, and that microdischarge may be statistically small even when the number of particles participated in it is large (tens of thousands).

For illustration, let us say the ramp rate is $3\ \mathrm{V}/\mu\mathrm{s}$, which requires about $N\sim 20\,000$ ions in the gap to sustain this current (for the "test" cell). With effective secondary emission coefficient $\gamma$ of 0.5 the deviation of ions in the gap from one generation to another is about $\delta N\sim(N/\gamma)^{1/2}\sim 200$, which is about 1% of the total number of ions. On the other hand, if $\gamma\sim 0.005$, then $\delta N\sim 2000$, or 10%, and since in minima relative fluctuations are even larger, they can lead to a catastrophic disruption of the discharge, as shown in Figs. 4 and 5. Apparently larger fluctuations also lead to a shorter "life" and thus to a less stable discharge. For the cases shown in Fig. 5 we have chosen 93% Ne+7% Xe mixtures (common for plasma displays), with two different values for the xenon secondary emission coefficient. Oscillations are being observed in both of these cases, but in the case of large $\gamma$ they seemed to be bound within some limits, at least for some time.

As we said before, both fluid and statistical features are clearly present in the ramp, as well as in any Townsend discharge. The fluid nature of the discharge is presented in the current (number of particles) oscillations, when the discharge is off the balance, and statistical nature is presented in the fluctuations leading to a "diffusion" of the "particle" (see

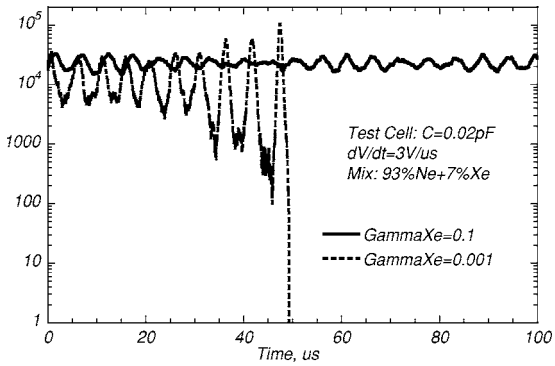


FIG. 5. Both discharges start with "ideal" initial conditions, and have $\langle N\rangle\approx 20\,000$. Discharge with small $\gamma_{\mathrm{Xe}}$ demonstrates much larger fluctuations and oscillations. In both cases the vacuum value of $\gamma_{\mathrm{Ne}}$ is 0.64.

Sec. II) between different phase trajectories (or "energies") leading to irregular increase or decrease of the amplitude of the oscillations. In the absence of any decay mechanism, the discharge is unstable, since such diffusion will sooner or later result in its disruption ($N<1$). We call this kind of instability statistical instability to distinguish it from a regular kind of instability, with exponential growth of the fluctuations. One can qualitatively describe this instability assuming that change of the particles in the gap in one generation of ions is small: $\Delta_T\ll 1$ and $\gamma N\ll 1$. One may write then

$$\bar{q}=q+(\tau_i\tau_r\omega_0^2)p+ae^{-q/2}r/\sqrt{\gamma\langle N\rangle}, \tag{22}$$

where $\bar{q}$ is the number of ions in the following generation [$\bar{q}=q(t+\tau_i)$, $q\equiv\ln(N/\langle N\rangle)$], and we used parameters $\tau_r=V_{\mathrm{br}}/\lambda$—the characteristic ramp time, $\omega_0$—frequency of small oscillations, and $\tau_i$—ion transit time instead of $\kappa$, $\lambda$ and $L$ (see Sec. II). Coefficient $a\sim 1$, and $r$ is a random number, $\langle r\rangle=0$, $\langle r^2\rangle=1$.

$$\bar{p}=p+(\tau_i/\tau_r)(1-e^{-\bar{q}}), \tag{23}$$

where $\bar{p}=p(t+\tau_i)$. Equations (22) and (23) are written in the way that conserves canonicity of the original equations (8) in the absence of fluctuations ($a=0$).[15] One can check that Jacobian $J\equiv\partial(\bar{p},\bar{q})/\partial(p,q)=1$. When $a\neq 0$ in the last term of Eq. (22), the Jacobian is no longer equal to 1,

$$J=1-ae^{-q/2}(r/2)/\sqrt{\gamma\langle N\rangle}. \tag{24}$$

Since $J$ characterizes the ratio of integrals

$$I(W)=\oint pdq \tag{25}$$

calculated along appropriate trajectories containing coordinates $(\bar{p},\bar{q})$, and $(p,q)$, respectively, fluctuations of $J$ or $I(W)$ reflect fluctuations of the energy $W$ at each time step $\tau_i$ and thus some kind of diffusion of the energy. Sooner or later this diffusion will bring the system to the phase trajectory which has less than one ion in the gap (in the minimum) and discharge will die, unless diffusion coefficient turns to zero at some energy. In order to estimate the diffusion it is convenient to rewrite the last equation in terms of energy. As we already mentioned before, the left hand side of Eq. (24) is

$$J = \frac{I(\bar{W})}{I(W)} = 1 + \delta W \frac{\partial I(W)/\partial W}{I(W)} = 1 + \delta W \frac{T(W)}{I(W)}, \tag{26}$$

where $\delta W = \bar{W} - W$, and we used that the period of oscillations $T$ [see Eq. (11)] and $I(W)$ are related,

$$T(W) = \frac{\partial}{\partial W} \oint p dq \equiv \frac{\partial I(W)}{\partial W}. \tag{27}$$

The energy dependence in the right hand side of Eq. (24) comes from the exponent containing $q = q(W,p)$. For low energies absolute values of $q$ are also small and one can ignore the exponent. For large energies, and large magnitudes of $|q|$ one can write $q = (q - q_{\min}) + q_{\min}$, and using solution for large $|q_{\min}|$; $W = -q_{\min}/\tau_r$, one obtains

$$e^{-q/2} \sim e^{W\tau_r/2} e^{(q_{\min}-q)/2}. \tag{28}$$

For small energies $T = \text{const}$, $I(W) = TW$, we obtain

$$\delta \ln W \sim a \frac{r}{\sqrt{4\gamma\langle N\rangle}}. \tag{29}$$

Here and below we "dropped" the unnecessary minus sign in the right hand side, because the sign of the term is determined by the random number $r$.

Equation (24) written in the form of Eq. (29) describes a Brownian motion (along the coordinate $\ln W$) with diffusion coefficient $D \sim a^2/(4\gamma\langle N\rangle)$, so that

$$\ln^2[\Delta W/W(0)] \sim (a^2/\gamma\langle N\rangle)(t/\tau_i), \tag{30}$$

where $\Delta W$ is the energy spread due to this "motion" and

$$t/\tau_i \sim (\langle N\rangle \gamma/a^2) \ln^2[\Delta W/W(0)]. \tag{31}$$

If for $\Delta W$ we use the energy related to oscillation with $|q_{\min}| = 1$, and for $W(0)$ the energy $W_{\min} \approx 1/(\tau_r \gamma\langle N\rangle)$, which the system can obtain in a single step from $W = 0$, then it gives the time $t_{D1}$ required for oscillation to grow to large amplitude from any initial conditions.

$$t_{D1}/\tau_i \sim (\langle N\rangle \gamma/a^2) \ln^2(\gamma\langle N\rangle). \tag{32}$$

For large energies ($|q_{\min}| > 1$), we can still use $T/I(W) \sim 1/W$ and after transferring all terms containing $W$ into the left side we obtain

$$\delta W \frac{e^{-W\tau_r/2}}{W} \sim e^{(q_{\min}-q)/2} \frac{ar}{\sqrt{4\gamma\langle N\rangle}}. \tag{33}$$

The left hand side of this equation is the variation of the incomplete Gamma function $\Gamma(0, W\tau_r/2)$, and in the right hand side of it for the estimate we will replace the exponent $\exp[(q_{\min} - q)/2]$ with a step function $\eta[(q_{\min} - q)/2]$: $\eta(x \leqslant 1) = 1$ and $\eta(x > 1) = 0$. Then Eq. (33) takes again the form of equation describing the Brownian motion [along coordinate $\Gamma(0, W\tau_r/2)$] when $|q_{\min} - q| \leqslant 2$, and $W = \text{const}$ outside this range;

$$\delta\Gamma(0, W\tau_r/2) \sim \eta[(q_{\min} - q)/2] \frac{ar}{\sqrt{4\gamma\langle N\rangle}}. \tag{34}$$

Assuming that $\gamma\langle N\rangle$ is large and it takes many oscillation periods for the discharge to die (reach energy $W_{\max}\tau_r \geqslant \ln\langle N\rangle$), one can obtain from Eq. (34) for the spread

$$\Delta\Gamma^2(0, W\tau_r/2) \sim \frac{a^2}{\gamma\langle N\rangle} \frac{N_{\text{osc}}}{\omega_0\tau_i}. \tag{35}$$

Here we used the number of steps $4/(\omega_0\tau_i)$ along the trajectory during one current oscillation, which has $|(q_{\min} - q)/2| < 1$, and the number of current oscillations $N_{\text{osc}}$ instead of the number of total time steps $t/\tau_i$, as we did previously in Eq. (30). Using that $\Gamma(0,x)$ at large $x$ behaves as $e^{-x}/x$, and thus $\Gamma(0, W_{\max}\tau_r/2) \ll \Gamma[0, W(0)\tau_r/2]$, and choosing $W(t=0) = W(|q_{\min}| = 1)$ one can estimate the number of large amplitude current oscillations until they grow so much that discharge may die in any of them,

$$N_{\text{osc}} \sim \omega_0\tau_i(\gamma\langle N\rangle/a^2). \tag{36}$$

As we already discussed, most of this time (oscillations) is spent at the lower energies, where the period of oscillations is about $T \sim 2\pi/\omega_0$. This agrees with our estimates of the relative fluctuation $\delta N/N \sim 1/\sqrt{\gamma N}$, which increases with the energy. Comparing times given by Eqs. (32) and (36) one finds that it takes about

$$t \sim t_{D1} \sim \tau_i(\gamma\langle N\rangle/a^2) \ln^2(\gamma\langle N\rangle) \tag{37}$$

for oscillations to grow (diffusively) from zero to the maximum amplitude, when discharge may die.

One should keep in mind that the condition $\langle r\rangle = 0$ is valid only when the number of terms (events) in the appropriate sum is very large; on the other hand there is only about $1/(\omega_0\tau_i)$ number of such terms during the full oscillation period, which make contribution to the "energy" drift. This means that only high frequency harmonics ($\omega > \omega_0$) of the fluctuation spectrum will cancel each other, but all other will not, and most likely the convective term, proportional to the sum $\Sigma r$ with only $1/(\omega_0\tau_i)$ terms, will differ from zero (and depends on specific random sequence), which means that transition between trajectories can be significantly faster than pure diffusive one, and it may take even less time for discharge to die than given by Eq. (37). The other thing to remember is that Brownian motion describes only the possibility of reaching some coordinate rather than exact coordinate, so different random sequences (random number generators or random seed numbers) will result in different lengths of the discharge.

Figure 6 show $N(t)/\langle N\rangle$, and the phase trajectory $p(q)$ (see Fig. 2) according to Eqs. (22) and (23), with initial conditions $q(t=0) = 0$, $p(t=0) = 0$, and $\langle N\rangle = 60\,000$, $\gamma = 0.001$. It took only ~200 steps ($\tau_i$) for the discharge to reach the amplitude, when it could die in one step, while according to our estimate [Eq. (37)] it would take around 1000 steps. One possible reason for this is that the spectrum of the sequence produced by the random number generator, which has a low frequency component, has a drift component for short sequences of $1/(\omega_0\tau_i)$ terms.

Despite its simplicity and apparent incompleteness, the results from this model [Eqs. (22) and (23)] are quite close to those obtained in 3D PIC/Monte Carlo simulations (compare Fig. 6 with Figs. 4 and 5), even the numbers of time steps

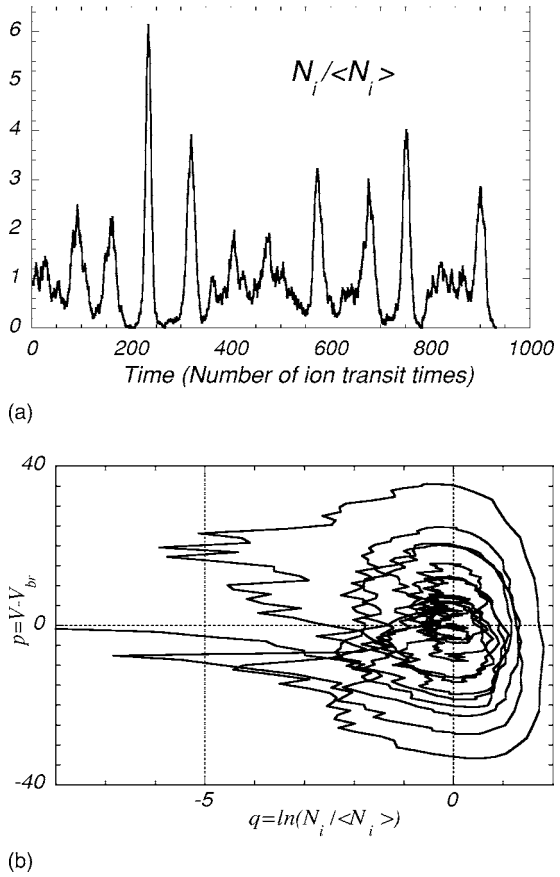


FIG. 6. Numerical solution of Eqs. (22) and (23), with initial conditions $q(t=0)=0$, $p(t=0)=0$, $\langle N\rangle \approx 60\,000$, and $\omega_0\tau_i \approx 0.06$. Fluctuations near the minimum of the current peaks are large and sooner or later one of them leads to discharge disruption.

($\tau_i \sim 100$ ns) for the growth of oscillations are close, which proves that this model indeed catches the essence of this instability.

## IV. STABILIZING A TOWNSEND DISCHARGE: EXTERNAL SOURCES

As we have shown in the previous section, the Townsend or ramp discharge in a PDP is not sustainable. As no charged particles are left in the cell, the only way to restart discharge again is through an additional independent source of electrons or ions. There is a variety of different sources, and the importance of one or another depends on the specifics of any particular system. Depending on the nature of a source, it has different spatial and temporary characteristics, and thus may be more or less effective. For example, if this source is due to the metastables produced in this discharge, then their spatial distribution repeats electron distribution and thus proportional to $e^{-\alpha z}$, where $z$ is the distance from the anode, so the spatial distribution corresponding to this source is concentrated near the anode ($\propto e^{-2\alpha z}$), and electrons produced by this source practically do not produce any more ionizations. On the other hand if the external source is caused by electron exoemission,[9–11] from the cathode surface, then each electron starts an avalanche, which produces about $e^{\alpha L} \sim 1/\gamma \gg 1$ ions (pairs) in the gap. Clearly one needs to use some unified way to investigate the effect of these sources. For convenience we will consider only exoemission of electrons from the cathode area—any other source can be recalculated to such a source with appropriate intensity, so that together with avalanches resulting from the original source it produces the same number of electron-ion pairs in the volume as the one associated with exoemission. In this paper we will not discuss the nature of exoemission, but simply use the fact that this process exists. In the simulations shown below it is imitated by a random emission of electrons (with specified average rate) from a random position on the cathode surface.

While in our simulations described in the previous section, we have used "good" initial conditions, when one could expect that fluctuations are small at least in the beginning of the discharge, the point of this section is to show the possible stabilization of the discharge, so we start all simulations with the worst scenario, assuming that there are no charged particles in the volume (at $t=0$).

Obviously, if exoemission is weak, then discharge may actually die, then start again, then die, etc. [see Fig. 7(a)]. In this case discharge may have very large peaks, and the voltage across the gap before and after peak may differ by 10–20 V. If exoemission is strong enough, so that the surface emits electron before the last ion left the volume, then the discharge never dies. Such a role of external sources is qualitatively different from what we obtained in the fluid approximation (Sec. II). In the presence of fluctuations the steady discharge current is statistically unstable, but when the amplitude of oscillations grows so much that electron current in the minimum of the oscillation is about the one produced by the source, fluctuations become asymmetric-those leading to the discharge extinguishing cannot make the current smaller than the one provided by the source, but those leading to the growth of the current are not limited. This results in the effective decay of the large amplitude current oscillations. Obviously, the larger the source, the lower the amplitude of the oscillations.

The plots of the ion density during the ramps in the 1D test cell are the same with those we have used in the previous simulations, but in the presence of the exoemission from the cathode are shown in Fig. 7. We started every simulation with no charged particles in the volume, and chose the ramp rate of 3 V/$\mu$s. We used mixture of 93%Ne+7%Xe, and assumed that $\gamma_{Xe}=0.001$—the case that would certainly be unstable without exoemission. The initial voltage was chosen slightly below the breakdown voltage, so until the voltage across the gap exceeded $V_{br}$ the number of ions in the gap stayed too low to be seen in some of these figures.

## V. SUMMARY

The stability of a dynamical system is usually associated with an exponential growth or decay of small fluctuations. So as long as such growing modes do not exist the system is considered of being stable. Based on such a view, the Townsend discharge, the dynamics of which in the fluid approximation can be described by the same equations as a nonharmonic oscillator must be stable—a fluctuation causes a nongrowing oscillation which decays in the presence of any additional external source. This work, however, shows

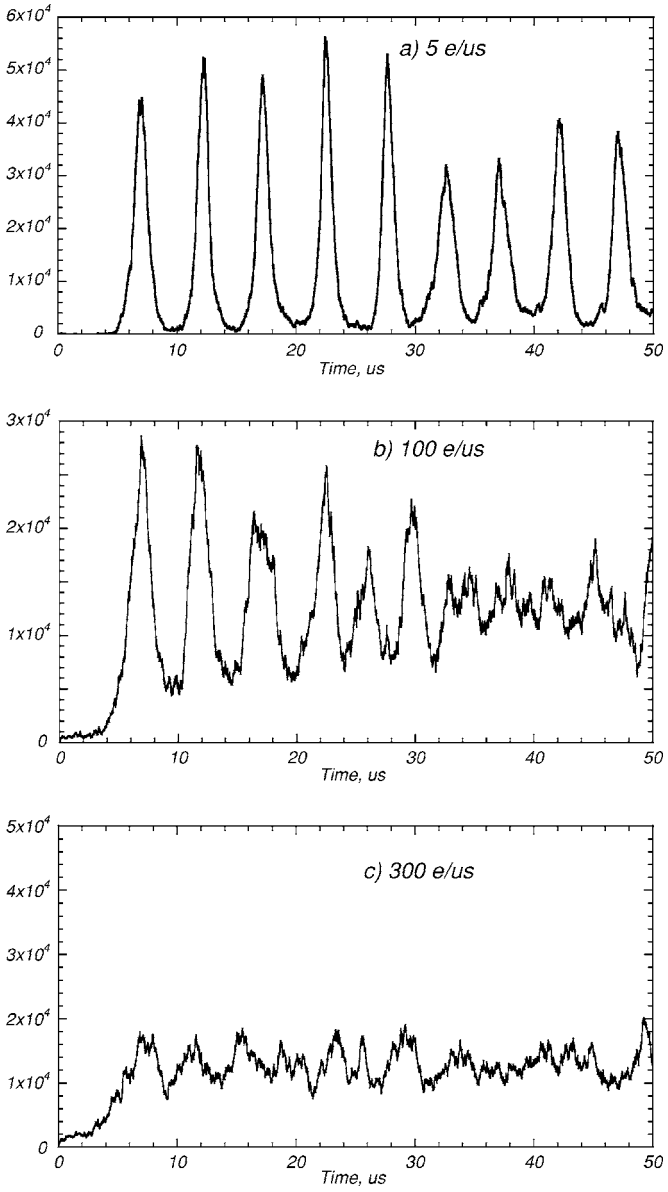


FIG. 7. 1D Monte Carlo simulations of the exoemission in the "test" cell. We choose 93%Ne+7%Xe mixture for comparison with previous results. Low exoemission rate results in many separate, not sustainable discharges, some of which are very strong. With increasing the exoemission rate, oscillations of the ion density decrease, and discharge becomes stable. Initially, no charged particles are assumed in the gap.

that under certain conditions the large number of uncorrelated fluctuations may lead to a significant change of the "energy" of the discharge oscillations, which in the discharge with a limited number of charged particles may result in the extinguishing of that discharge. One of these conditions is that the system must have a "long memory"—so that effects caused by a series of fluctuations may accumulate. This condition is automatically satisfied in conservative systems such as the Townsend discharge. The other factor strongly affecting the development of this instability is a feedback from the oscillations initiated by the fluctuations. Oscillations make fluctuations unequal—those occurred in the minimum of the current have significantly larger weight than the others, and thus statistically a small number of fluctuations controls the development of the discharge.

Fluctuations associated with ionization and secondary emission processes clearly change the role of external sources and initial conditions for the microdischarge. In the absence of fluctuations (fluid approximation), good initial conditions guarantee a small amplitude of oscillations, and external sources provide their decay. In a small system with fluctuations initial conditions play much less of a role, because the steady state is statistically unstable, and large current oscillations leading to the disruption of the discharge will appear at any initial conditions. On the other hand, sources not only damp large oscillations, but also limit their amplitude.

Statistical effects similar to those investigated in this paper are obviously not unique to a one-dimensional Townsend discharge. Earlier we investigated it numerically in the geometry of a plasma display cell[16,17] and one can imagine many other discrete systems (e.g., biological or financial), dynamics of which can be approximated by Hamiltonian equations where large slowly decaying (or not decaying) fluctuations are not rare.

The one-dimensional model developed here, which uses only one component of electric field independent of transverse coordinates, is not valid in large systems, where nonuniformities of electric field (in the transverse directions) caused by different currents may appear. These nonuniformities together with electron diffusion will result in interaction between different regions of the discharge effectively making up sources necessary for stabilization of the discharge. These kinds of effects will be investigated later.

## ACKNOWLEDGMENTS

The author is grateful to M. Molotskii for a number of conversations regarding exoemission, and V. N. Khudik for useful discussions.

## APPENDIX

Equations describing the electron and ion currents with ac count of additional source $S$ are as follows:

$$\frac{\partial n_e}{\partial t} + \frac{\partial \varphi_e}{\partial z} = -\alpha(E)\varphi_e + S, \tag{A1}$$

$$\frac{\partial n_i}{\partial t} + \frac{\partial \varphi_i}{\partial z} = -\alpha(E)\varphi_e + S, \tag{A2}$$

where $\varphi_{e,i}$ is the electron and ion fluxes, respectively, $\varphi_{e,i} \equiv (nv)_{e,i}$. For all slow compared to electron time processes, one can neglect $\partial n_e/\partial t$ compared to other terms in (A1). Using the boundary condition at the cathode

$$\varphi_e(L,t) = -\gamma\varphi_i(L,t), \tag{A3}$$

one obtains

$$\varphi_e(z,t) = -\gamma\varphi_i(L,t)e^{\alpha(L-z)} + e^{-\alpha z}\int_z^L S(z')e^{\alpha z'}dz'. \tag{A4}$$

Substituting this solution into (A2) gives for $\varphi_i(z,t)$

$$\varphi_i(z,t) = -\int_0^z \alpha[t-\tau(z,z')]\varphi_e[z',t-\tau(z,z')]dz' + \int_0^z S[z',t-\tau(z,z')]dz', \quad \text{(A5)}$$

where $\tau(z,z')=(z-z')/v_i$. Choosing $z=L$, expanding $\varphi_e(z,t-\tau)=\varphi_e(z,t)-\tau\partial\varphi_e(z,t)/\partial t$, and assuming that $|\partial \ln \varphi_i(L,t)/\partial t| \gg |\partial \ln S(L,t)/\partial t|, |\partial \ln \alpha/\partial t|$, we obtain

$$\varphi_i(L,t) = -\int_0^L \alpha\left[-\gamma\varphi_i(L,t)e^{\alpha(L-z)} + e^{-\alpha z}\int_0^L e^{\alpha z'}S(z',t)dz'\right]dz - \alpha\gamma\frac{\partial\varphi_i(L,t)}{\partial t}\int_0^L e^{\alpha(L-z)}\tau(L,z)dz + \int_0^L S(z,t)dz.$$

Combining together similar terms, and integrating we obtain

$$\bar{\tau}\frac{\partial\varphi_i(L,t)}{\partial t} = \Delta_T\varphi_i(L,t) + \int_0^L e^{\alpha z}Sdz,$$

where

$$\bar{\tau} = \gamma\int_0^L \alpha\frac{L-z}{v_i}e^{\alpha(L-z)}dz \approx \frac{L}{v_i}.$$

Using that for slow processes $j=(1+\gamma)j_i(L,t)=(1+\gamma)e\varphi_i(L,t)$, and expanding the coefficient before $\varphi_i(L,t)$ near the breakdown we obtain Eq. (14)

$$\frac{\partial j}{\partial t} = \frac{\kappa}{L}(V-V_{\mathrm{br}})j + e\frac{v_i}{L}\hat{S}, \quad \text{(A6)}$$

where

$$\hat{S} = \frac{1+\gamma}{\gamma F(\alpha L)}e^{-\alpha L}\int_0^L e^{\alpha z}Sdz \quad \text{(A7)}$$

and $F(\alpha L)=(\alpha L-1+e^{-\alpha L})/(\alpha L)$. In case $\gamma \ll 1$, $F(\alpha L)\sim 1$, $\gamma e^{\alpha L}\sim 1$, and $\hat{S}\approx\int_0^L e^{\alpha z}Sdz$.


[1] L. F. Weber, Asia Display '98 Digest, 15–27 (1998) .
[2] V. P. Nagorny, P. J. Drallos, and L. F. Weber, SID Int. Symp. Digest Tech. Papers **31**, 114 (2000).
[3] Yu. S. Akishev, A. V. Dem'yanov, V. B. Karal'nik, M. V. Pan'kin, and N. I. Trushkin,Plasma Phys. Rep. **27**, 164 (2001)..
[4] L. Mangolini, K. Orlov, U. Kortshagen, J. Heberlein, and U. Kogelschatz,Appl. Phys. Lett. **80**, 1722 (2002).
[5] I. Radu, R. Bartnikas, and M. R. Wertheimer, IEEE Trans. Plasma Sci. **31**, 1363 (2003).
[6] Yu. B. Golubovskiil *et al.*, J. Phys. D **36**, 39 (2003).
[7] V. N. Khudik and A. Shvydky, GEC'2003, available at www.plasmadynamics.com
[8] V. P. Nagorny, P. J. Drallos, and W. Williamson, Jr., J. Appl. Phys. **77**, 3645 (1995).
[9] L. Oster, V. Yaskolko, and J. Haddad, Phys. Status Solidi A **174**, 431 (1999).
[10] L. Oster, V. Yaskolko, and J. Haddad, Phys. Status Solidi A **187**, 481 (2001).
[11] M. Molotskii, M. Naich, and G. Rosenman, J. Appl. Phys. **94**, 4652 (2003).
[12] V. N. Khudik, V. P. Nagorny, and A. Shvydky, J. Appl. Phys. **94**, 6291 (2003).
[13] V. P. Nagorny and P. J. Drallos, Plasma Sources Sci. Technol. **6**, 212 (1997).
[14] V. A. Shveigert, High Temp. **27**, 195 (1989).
[15] B. V. Chirikov, Particle Dynamics in Magnetic Traps, in *Reviews of Plasma Physics*, edited by B. B. Kadomtsev (Consultants Bureau, New York, NY, 1987), Vol. 13, pp. 1–91.
[16] V. P. Nagorny, V. N. Khudik, P. J. Drallos, A. Shvydky, *Asia Display/IMID 2005 Digest*, 155–160 (2005); available at www.plasmadynamics.com
[17] V P. Nagorny, V. N. Khudik, and A. Shvydky, IEEE Trans. Plasma Sci. **34**, 343 (2006).